Journal of Colloid and Interface Science 424 (2014) 22–26

Contents lists available at ScienceDirect

Journal of Colloid and Interface Science

www.elsevier.com/locate/jcis

Preparation of porous diatomite-templated carbons with large adsorption capacity and mesoporous zeolite K-H as a byproduct

Dong Liu [a], Weiwei Yuan [a,b], Liangliang Deng [a,b], Wenbin Yu [a,b], Hongjuan Sun [c], Peng Yuan [a,*]

[a] CAS Key Laboratory of Mineralogy and Metallogeny, Guangzhou Institute of Geochemistry, Chinese Academy of Sciences, Guangzhou 510640, China
[b] University of Chinese Academy of Sciences, Beijing 100049, China
[c] Southwest University of Science and Technology, Mianyang, Sichuan 621010, China

ARTICLE INFO

Article history:
Received 8 November 2013
Accepted 1 March 2014
Available online 12 March 2014

Keywords:
Diatomite-templated carbon
KOH activation
High porosity
Methylene blue adsorption
Zeolite K-H

ABSTRACT

In this study, KOH activation was performed to enhance the porosity of the diatomite-templated carbon and to increase its adsorption capacity of methylene blue (MB). In addition to serving as the activation agent, KOH was also used as the etchant to remove the diatomite templates. Zeolite K-H was synthesized as a byproduct via utilization of the resultant silicon- and potassium-containing solutions created from the KOH etching of the diatomite templates. The obtained diatomite-based carbons were composed of macroporous carbon pillars and tubes, which were derived from the replication of the diatomite templates and were well preserved after KOH activation. The abundant micropores in the walls of the carbon pillars and tubes were derived from the break and reconfiguration of carbon films during both the removal of the diatomite templates and KOH activation. Compared with the original diatomite-templated carbons and CO_2-activated carbons, the KOH-activated carbons had much higher specific surface areas (988 m^2/g) and pore volumes (0.675 cm^3/g). Moreover, the KOH-activated carbons possessed larger MB adsorption capacity (the maximum Langmuir adsorption capacity: 645.2 mg/g) than those of the original carbons and CO_2-activated carbons. These results showed that KOH activation was a high effective activation method. The zeolite K-H byproduct was obtained by utilizing the silicon- and potassium-containing solution as the silicon and potassium sources. The zeolite exhibited a stick-like morphology and possessed nanosized particles with a mesopore-predominant porous structure which was observed by TEM for the first time.

1. Introduction

Hierarchically porous carbons are attracting attention due to the presence of macropores or mesopores in microporous carbons, which can improve the transport of adsorbed molecules through the porous framework of carbons [1–3]. Recently, hierarchically porous carbons with unique macroporous carbons have been prepared using diatomite template [4–8], which is a natural biogenetic mineral derived from an assemblage of diatom shells and is of highly developed macroporosity [9–17].

The diatomite-templated carbons possess macropores, mesopores and micropores which are mainly derived from the replication of the diatomite templates, the stacking of carbon species and the breaking of carbon films during the removal of diatomite templates, respectively [4,5,7]. Previous studies have evaluated the adsorption capacity of diatomite-templated carbons for gas and liquid molecules using H_2 and methylene blue (MB), respectively, as model molecules [5,6]. However, the adsorption capacities were ordinary due to the low specific surface area (S_{BET}) and micropore volume (V_{micro}) of the diatomite-templated carbons.

In our recent study, physical activation with CO_2 or H_2O as the activation agent was performed to enhance the porosity of diatomite-templated carbons and further to increase their adsorption capacities [18]. After activation, abundant micropores were generated in the walls of the carbon pillars and tubes of diatomite-templated carbons, and the S_{BET} and V_{micro} values of the products were significantly increased. CO_2 activation was more effective than H_2O activation. The MB adsorption capacity of the CO_2-activated carbons was over 2 times larger than those of the original carbons. In addition to physical activation, chemical activation using chemical activation agents (KOH, NaOH or H_3PO_4) is demonstrated to be effective and has been widely used to enhance the porosity of carbon materials [19–21]. Compared with physical activation, chemical activation is of some advantages, such as a lower required

* Corresponding author. Address: Guangzhou Institute of Geochemistry, Chinese Academy of Sciences, Wushan, Guangzhou 510640, China. Fax: +86 20 85290341.
E-mail address: yuanpeng@gig.ac.cn (P. Yuan).

http://dx.doi.org/10.1016/j.jcis.2014.03.001
0021-9797/

activation temperature, a shorter activation time and the production of carbon materials with higher porosity [20,22,23]. Because of the higher activation capability for enhancing the porosity of carbons than that achieved with some other chemical activation agents, KOH is universally used as the chemical activation agent [21,24–27]. However, until now, no reports have described KOH activation of diatomite-templated carbons; the activation effects and the influence of activation on the surface porosity and adsorption capacity of the carbons remain unclear, even though this information would aid in the practical application and industrial production of these carbons.

In the present work, KOH was used as the activation agent to enhance the porosity and to increase the adsorption capacity of diatomite-templated carbons which were prepared using inherent acid sites of the diatomite as a catalyst. The activation effects and the influence mechanism of KOH activation on the porosity, framework and MB adsorption capacity of the carbons were investigated. Moreover, KOH is proposed to be an effective etchant for the removal of the siliceous templates [28,29], and KOH etching is of the lower potential threats to environment and health of researchers and higher reusability of the obtained silicon-containing solution, compared to HF etching. Therefore, KOH was also utilized to remove the diatomite templates in this study. Zeolite K-H as a byproduct was prepared using the resulting silicon- and potassium-containing solution recycled from the KOH etching of diatomite templates for the purpose of recycling and further utilization.

2. Materials and methods

2.1. Diatomite

Diatomite was obtained from Qingshanyuan Diatomite Co., Ltd. (Jilin provinces, China). The dominant diatoms in the diatomite were of the genus *Coscinodiscus* Ehrenberg (Centrales) and were disk-shaped with a highly developed macroporous structure. The diatomite samples were purified via sedimentation [5], and the purified samples were denoted as Dt (for the chemical compositions, see Supplementary Data).

2.2. Preparation of the activated diatomite-templated carbon and zeolite

The porous carbon product was prepared as follows: diatomite and furfuryl alcohol ($C_5H_6O_2$, ⩾98 wt%, Sigma–Aldrich Co. LLC) were mixed in ceramic boats with a solid/liquid ratio of 1 g:5 mL, and then stirred for 1.5 h at room temperature, followed by heating at 95 °C for 24 h. The mixture was further heated at 150 °C under vacuum conditions for 1 h to promote cross-linking. It was then transferred into a tubular oven and heated at 700 °C for 3 h under a N_2 atmosphere (99.999%) for complete carbonization. The resulting products (6 g) were dissolved in 22 mL KOH (⩾85 wt%, Sinopharm Chemical Reagent Co., Ltd., China; abbreviated as SCR hereafter) solution with the concentration of 4 mol/L at 80 °C and vigorously stirred for 91 h.

The mixture was separated via centrifugation: (1) the obtained solid was dried at 60 °C for 12 h, followed by heating at 600 °C for 3 h in the tubular oven under the N_2 atmosphere. The products were washed with deionized water, centrifuged for 3 times and placed in the 36.5 wt% HCl solution (SCR) at 80 °C for 24 h. The solid was then separated and washed repeatedly with deionized water until it was free of Cl^- (as determined using $AgNO_3$ from SCR). The material was subsequently dried at 60 °C for 12 h. The dried solid was denoted as C/Dt-KOH. (2) The obtained supernatant was placed in a flask to which 15.20 mL of H_2O was added. Under vigorous stirring, 15.50 mL tetrapropylammonium hydroxide (TPAOH, 25 wt%, SCR) was added dropwise. After being stirred for 24 h at room temperature, the mixture was heated at 100 °C for 72 h in a reflux unit. The solid, which was obtained via centrifugation was washed with deionized water, dried at 80 °C and heated at 550 °C for 6 h. The derived solid was denoted as Z/Dt. All chemicals and reagents used in this process were of analytical grade (AG) and were used as received.

2.3. Characterization methods

The X-ray diffraction (XRD) patterns were taken on a Bruker D8 advance diffractometer with Ni filter and Cu K*a* radiation (λ = 0.154 nm) with a generator voltage of 40 kV and a generator current of 40 mA. A scan rate of 1° (2θ)/min was used for measurements. The detections were performed at relative humidity lower than 40% at approximately ~25 °C.

Scanning electron microscopy (SEM) micrographs were obtained using a 5 kV FEI-Sirion 200 field emission scanning electron microscope attached to an Oxford INCA energy dispersive X-ray spectroscopy (EDS). The detections were performed at the pressures $\leqslant 1 \times 10^{-5}$ Pa and at the ambient temperature of 20–23 °C.

Transmission electron microscopy (TEM) images were obtained on a JEOL JEM-2100 electron microscope operated at an acceleration voltage of 200 kV with the pressures of 1×10^{-6} to 1×10^{-7} Pa at the ambient temperature of 23 °C. The specimens for TEM observation were prepared as follows: the sample was ultrasonically dispersed in ethanol for 5 min, and then a drop of the sample suspension was placed onto a carbon-coated copper grid. The grid was allowed to stand for 10 min before being transferred into the microscope.

The N_2 adsorption–desorption isotherms were measured on a Micromeritics ASAP 2020 system (Micromeritics Co., Norcross, USA) at liquid nitrogen temperature (−196 °C). Prior to the measurement, the samples were outgassed at 150 °C for 12 h at the degas port and then transferred to the analysis port to degas under a relative pressure of 0.01 for additional 6 h. The S_{BET} value was calculated using the multiple-point Brunauer–Emmett–Teller (BET) method, and the total pore volume (V_p) was evaluated from the N_2 uptake at a relative pressure of approximately 0.99. The V_{micro} value was estimated using the HK method [30]. The micropore and mesopore size distributions, which ranged from 0.35 to 30 nm, were determined using non-local density functional theory (NLDFT) [31]. The analysis was repeated for 3 times, and all the finally reported values were the mean values.

The MB adsorption capacity of C/Dt-KOH was determined at ambient temperature (~25 °C) following the typical processes as described in our previous report [5], and tests were performed for 4 times. MB ($C_{16}H_{18}C_lN_3S_2{\cdot}3H_2O$, AG) used in the experiment was purchased from Tianjin Kermel Chemical Reagent Co., Ltd., China. The adsorption isotherm is simulated using the Langmuir model and the linear form of the Langmuir model is given as

$$\frac{C_e}{Q_e} = \frac{1}{k_L Q_m} + \frac{1}{Q_m} C_e \quad (1)$$

where k_L (L/g) and Q_m (mg/g) are the Langmuir constant and the monolayer adsorption capacity, respectively, and C_e (mg/L) is the equilibrium concentration of the MB solution.

The affinity between adsorbent and adsorbate is evaluated based on the separation factor, R_L, determined from the Langmuir adsorption isotherm model. R_L is defined by the following equation:

$$R_L = \frac{1}{(1 + k_L C_0)} \quad (2)$$

where C_0 (mg/L) is the initial concentration of MB and K_L (L/mg) is the Langmuir constant related to the energy of adsorption.

3. Results and discussion

3.1. KOH-activated carbons

The diatomite-templated carbons exhibited two broad XRD diffractions at approximately 23° and 44° (Fig. 1a), which were attributed to the (002) and (100) reflections of the graphite, respectively. The $d_{(002)}$ value, commonly used to estimate the graphitization degree of the carbon, was 0.387 nm and was larger than that of the ideal graphite (0.335 nm) [32]; this discrepancy indicates that the carbon products were composed of disorderly stacked graphite microcrystals rather than the complete graphite layers [33,34].

C/Dt-KOH exhibited unique tubular (Fig. 1b and the inset) and pillared (Fig. 1c) macropores, whose pore sizes were similar to those of the initial diatom shells (see Supplementary Data, Fig. S1). This suggests that the macropores were derived from the replication of the macroporous structures of diatom shells. The carbon tubes were derived from the edge macropores of diatom shells based on our previous studies (for the formation mechanisms, see our previous report [6]) and were hollow and interconnected with the thin carbon film through the planform (Fig. 1b). The carbon pillars derived from the central macropores were predominantly solid, but were hollow at both ends. These carbon tubes and pillars interconnected by the carbon films possessed similar morphology to the diatomite-templated carbon without activation (denoted as C/Dt), which was detailed described in our previous papers [5,6]. This result indicates that monolithic construction and morphology of diatomite-templated carbons were well preserved during KOH activation. Moreover, abundant micropores were observed in the walls of the carbon tubes and pillars These micropores were narrow slit-like with pore sizes smaller than 1 nm (Fig. 1d).

Similar to C/Dt, C/Dt-KOH exhibited type II adsorption isotherms with H3-type hysteresis loop of isotherms (Fig. 2a). The high N_2 adsorption capacity of C/Dt-KOH at the relative pressure near to zero indicates the existence of abundant micropores [40], which was in good agreement with the TEM result. And the N_2 adsorption capacity of C/Dt-KOH was much higher than that of C/Dt (Fig. 2a), implying that KOH activation was an efficient method in the increase in the carbons micropores. The sharp rise of the isotherm near the relative pressure of 1 indicates the existence of macropores in carbon products. H3-type hysteresis loop indicates the existence of mesopores [35] and reflects that the pores are mainly narrow and slit-like [34,35], which agrees well with TEM observation (Fig. 1d).

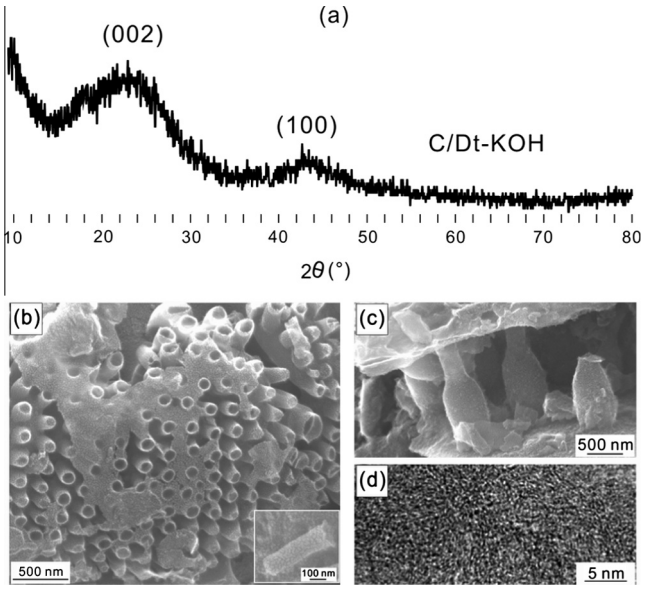

Fig. 1. (a) XRD pattern of C/Dt-KOH; SEM images of (b) carbon tubes of C/Dt-KOH (the inset: a single carbon tube) and (c) carbons pillars of C/Dt-KOH; (d) TEM image of micropores on carbon walls of C/Dt-KOH.

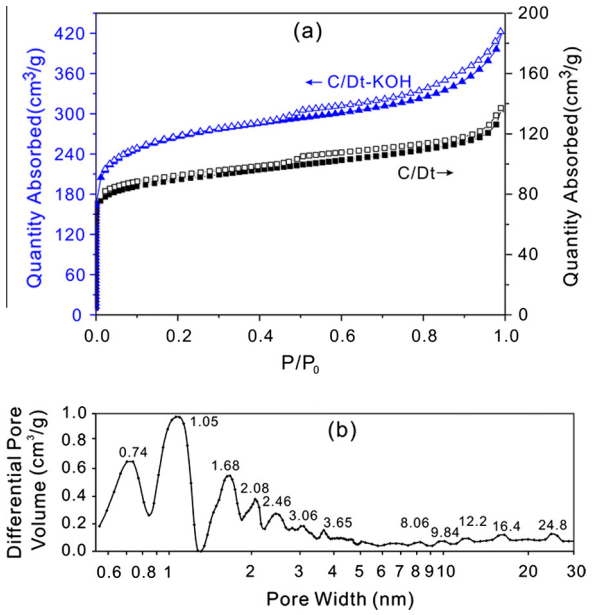

Fig. 2. (a) N_2 adsorption isotherms of C/Dt [5] and C/Dt-KOH; and (b) pore size distributions of C/Dt-KOH.

The mean S_{BET}, V_p and V_{micro} values of C/Dt-KOH were 988 m^2/g, 0.675 cm^3/g and 0.421 cm^3/g, respectively, and were more than three times larger than those of C/Dt (the mean S_{BET} value, 270 m^2/g; V_p value, 0.212 cm^3/g and V_{micro} value, 0.127 cm^3/g). The significant increase in the pore parameters indicates that KOH activation was an efficient method for enhancing the porosity of the diatomite-templated carbons. Moreover, the S_{BET} and V_p values of C/Dt-KOH were greater than those of the CO_2-activated diatomite-templated carbons (the mean S_{BET} value 886 m^2/g and V_p value, 0.658 [18]). It is noteworthy that the V_{micro} value of C/Dt-KOH was smaller than that of CO_2-activated carbons (V_{micro} value, 0.437 cm^3/g), which should be ascribed to the different activation mechanisms [20]. The difference in the increase in microporosity indicates CO_2-activation is more advantageous than KOH-activation. However, given its higher S_{BET} and V_p value and lower activation temperature, KOH activation was demonstrated higher efficiency and better economical viability than CO_2 activation.

Three populations existed at approximately 0.74, 1.05 and 1.68 nm (Fig. 2b) in the micropore size distribution region of C/Dt-KOH; and among them the 0.74 and 1.05 nm populations also appeared in the size distribution of C/Dt [5]. However, the volume of the 1.05 nm micropores of C/Dt-KOH was larger than that of C/Dt, indicating that some micropores with the pore size of 1.05 nm were derived from KOH activation. The appearance of 1.68 nm population after KOH activation was presumably attributed to the break and reconfiguration of adjacent 0.74 nm micropores during KOH activation. This attribution was based on the observation that C/Dt-KOH contained a smaller volume of 0.74 nm micropores than C/Dt. Moreover, several weak size distribution peaks were exhibited in the mesopore size region (Fig. 2b). These populations were attributed to the stacking of carbon particles [6] and reconfiguration of the broken adjacent micropores during KOH activation.

The MB adsorption isotherms for C/Dt-KOH (Fig. 3a) show that the adsorption capacity of the carbon increased with increasing MB

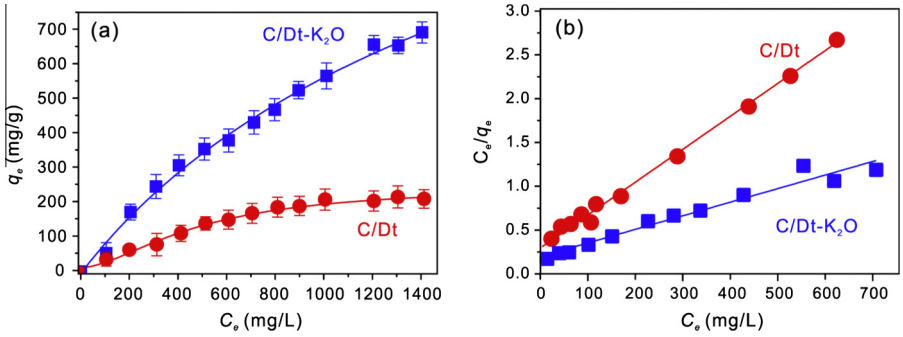

Fig. 3. The MB adsorption isotherms of C/Dt and C/Dt-KOH; and (b) linear fitting plots based on Langmuir isotherm model for MB adsorption.

concentration. The Langmuir isotherm model (R^2 = 0.9569) which fitted the experimental data better than Freundlich and Redlich–Peterson models (not showed) was used to quantitatively describe the adsorption data. The Langmuir adsorption capacity of MB on C/Dt-KOH (Q_m, mg/g) was 645.2 mg/g, which was calculated by the linear simulation of Langmuir isotherm model (Fig. 3b). This obtained value was much higher than that of C/Dt (250.0 mg/g) and also higher than that of CO_2-activated carbons [18]. The result indicates that KOH activation significantly increased the MB adsorption capacity of the diatomite-templated carbon. The increased MB adsorption capacity was attributed to the newly appeared pores during KOH activation. Moreover, the fact that the MB adsorption capacity of C/Dt-KOH was higher than that of CO_2-activated carbons implied the effect of KOH activation on the adsorption capacity was better.

R_L values (Eq. (2)) were traditionally used to estimate the affinity between MB and the carbons [36]. The R_L value of C/Dt-KOH ranged from 0.08 to 0.45, indicating the favorable MB uptake of these carbons [37].

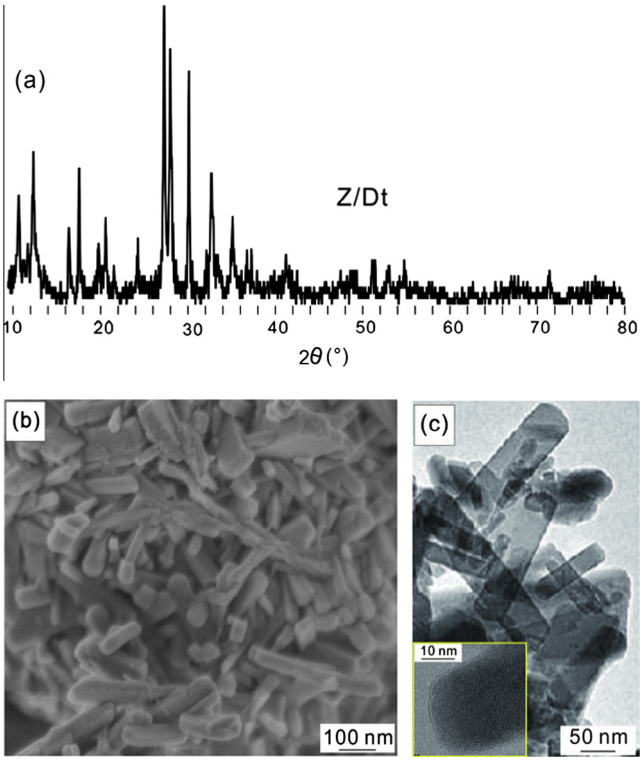

Fig. 4. (a) XRD pattern, (b) SEM image and (c) TEM image (the inset: porous morphology) of Z/Dt.

3.2. Zeolite byproduct

The XRD diffraction patterns of Z/Dt well matched those of zeolite K-H ($K_2Al_2Si_4O_{12}{\cdot}xH_2O$, Si:Al:K = 2:1:1 PDF#16-0692, from PCPDFWIN Software), which indicates that Z/Dt was zeolite K-H (Fig. 4a). These results demonstrate that the zeolite could be synthesized and the synthesis method was facile and economically feasible for the utilization of waste solutions from KOH-etched diatomite template and its simple processes under mild reaction conditions, such as the low temperature and pressure. The Si:Al:K ratio of Z/Dt obtained via EDS was 1.88:1:0.95, which was consistent with the formula for zeolite K-H and the previously reported result (1.98:1:0.82) in the previous report [38]. It is noteworthy that the structure of zeolite K-H has remained unclear until now, and its structure type is still unknown [38,39]. Moreover, the exact formation mechanism of Z/Dt, such as the roles of the TPAOH template, has not been confirmed and requires further investigation.

Z/Dt possessed a stick-shaped morphology with nano-sized particles of 50–120 nm in length and 30–80 nm in diameter (Fig. 4b and c). Different with needle-like zeolite K-H obtained by microwave-assisted preparation [38], self-assembled aggregation of Z/Dt crystals did not occur. As displaced in Fig. 4c (the inset), a porous structure with a pore size of 1.5–5.0 nm existed in the Z/Dt particle. The porous morphology of zeolite K-H was observed using the TEM analysis for the first time. Z/Dt was proposed here to be a primarily mesoporous zeolite because its pore sizes were predominantly larger than 2.4 nm (Fig. 4c the inset). The unique porous

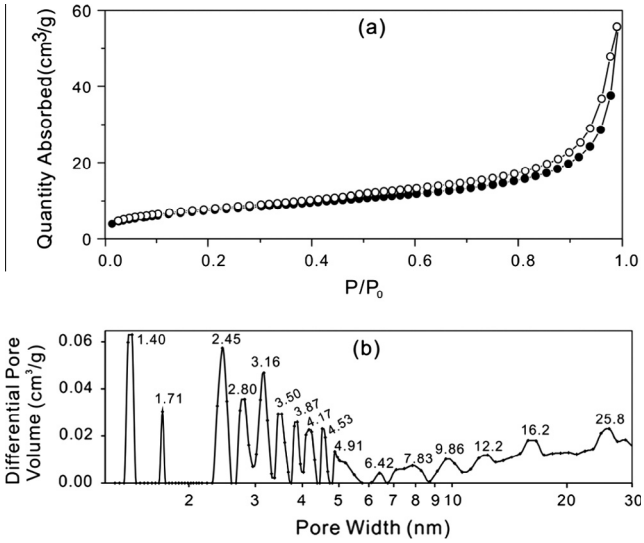

Fig. 5. N_2 adsorption isotherms (a) and pore size distributions (b) of Z/Dt.

structure implied a promising application of Z/Dt in catalysis [40,41] and adsorption of large-sized molecules [42].

Z/Dt exhibited type II adsorption isotherm with hysteresis loops, which indicates the presence of micropores and mesopores (Fig. 5a). The very low N_2 adsorption capacity of Z/Dt at a relative pressure approaching zero shows that very few micropores existed in Z/Dt, which was in good agreement with V_{micro} (0.012 cm^3/g) and the TEM results (Fig. 4c inset). The S_{BET} and V_p values of Z/Dt were 30 m^2/g and 0.089 cm^3/g, respectively. The mesopore volume (V_{meso}), which was calculated by subtracting V_{micro} from V_p, was 0.077 cm^3/g; this value was substantially larger than that of V_{micro}, which indicates the Z/Dt particles possessed a mesopore-predominate porous structure, as observed by TEM (Fig. 4c inset). The pore size distribution of Z/Dt shows that micropore sizes were centered at 1.40 and 1.71 nm and that mesopore sizes exhibited a wide distribution (Fig. 5b).

4. Conclusions

In this study, KOH activation, an effective activation method, was used to improve the porosity and the MB adsorption capacity of the diatomite-templated carbons. KOH activation resulted in the formation of new micropores and mesopores without destroying the morphology of original diatomite-templated carbons. The newly appeared micropores and mesopores existed in the walls of the carbon pillars and tubes replicated from diatom shell, and they were derived from the breaking and reconfiguration of carbon films during KOH activation. KOH-activated diatomite-templated carbons possessed the higher specific surface area (988 m^2/g), total pore volume (0.675 cm^3/g) and the MB adsorption capacity (645.2 mg/g) than those of the original carbons and CO_2-activated carbons.

Moreover, a facile and economically available method was used to prepare the zeolite K-H, during which the silicon- and potassium-containing solutions derived from the KOH-etched diatomite template were served as the silicon and potassium sources. The zeolite products possessed a stick-like morphology and nanosized particles with a mesopore-predominant porous structure, which was observed by TEM and confirmed by N_2 adsorption analysis for the first time.

Acknowledgments

The financial supports from the National Natural Scientific Foundation of China (Grant No. 41202024), the Team Project of Natural Science Foundation of Guangdong Province, China (Grant No. S2013030014241) and National Key Technology Research and Development Program of the Ministry of Science and Technology of China (Grant No. 2013BAC01B02) are gratefully acknowledged. This is a contribution (No. IS-1840) from GIGCAS.

Appendix A. Supplementary material

Supplementary data associated with this article can be found, in the online version, at http://dx.doi.org/10.1016/j.jcis.2014.03.001.

References

[1] C.D. Liang, Z.J. Li, S. Dai, Angew. Chem. Int. Ed. 47 (2008) 3696–3717.
[2] S. Alvarez, T. Valdes-Solis, A.B. Fuertes, Mater. Res. Bull. 43 (2008) 1898–1904.
[3] P. Adelhelm, Y.S. Hu, L. Chuenchom, M. Antonietti, B.M. Smarsly, J. Maier, Adv. Mater. 19 (2007) 4012–4014.
[4] M. Perez-Cabero, V. Puchol, D. Beltran, P. Amoros, Carbon 46 (2008) 297–304.
[5] D. Liu, P. Yuan, D.Y. Tan, H.M. Liu, T. Wang, M.D. Fan, J.X. Zhu, H.P. He, J. Colloid Interface Sci. 388 (2012) 176–184.
[6] D. Liu, P. Yuan, D.Y. Tan, H.M. Liu, M.D. Fan, A.H. Yuan, J.X. Zhu, H.P. He, Langmuir 26 (2010) 18624–18627.
[7] S.M. Holmes, B.E. Graniel-Garcia, P. Foran, P. Hill, E.P.L. Roberts, B.H. Sakakini, J.M. Newton, Chem. Commun. (2006) 2662–2663.
[8] X. Cai, G.S. Zhu, W.W. Zhang, H.Y. Zhao, C. Wang, S.L. Qiu, Y. Wei, Eur. J. Inorg. Chem. (2006) 3641–3645.
[9] M.W. Anderson, S.M. Holmes, N. Hanif, C.S. Cundy, Angew. Chem. Int. Ed. 39 (2000) 2707–2710.
[10] P. Yuan, D.Q. Wu, H.P. He, Z.Y. Lin, Appl. Surf. Sci. 227 (2004) 30–39.
[11] D. Losic, J.G. Mitchell, N.H. Voelcker, Adv. Mater. 21 (2009) 2947–2958.
[12] D. Losic, J.G. Mitchell, R. Lal, N.H. Voelcker, Adv. Funct. Mater. 17 (2007) 2439–2446.
[13] M.S. Aw, S. Simovic, J. Addai-Mensah, D. Losic, Nanomedicine 6 (2011) 1–15.
[14] H. Hadjar, B. Hamdi, M. Jaber, J. Brendlé, Z. Kessaïssia, H. Balard, J.B. Donnet, Micropor. Mesopor. Mater. 107 (2008) 219–226.
[15] M.A. Al-Ghouti, M.A.M. Khraisheh, M.N.M. Ahmad, S. Allen, J. Hazard. Mater. 165 (2009) 589–598.
[16] M.A. Al-Ghouti, Y.S. Al-Degs, Chem. Eng. J. 173 (2011) 115–128.
[17] P. Yuan, D. Liu, M.D. Fan, D. Yang, R.L. Zhu, F. Ge, J.X. Zhu, H.P. He, J. Hazard. Mater. 173 (2010) 614–621.
[18] D. Liu, W. Yuan, P. Yuan, W. Yu, D. Tan, H. Liu, H. He, Appl. Surf. Sci. (2013).
[19] C. Moreno-Castilla, F. Carrasco-Marın, M. Lopez-Ramon, M.A. Alvarez-Merino, Carbon 39 (2001) 1415–1420.
[20] J. Maciá-Agulló, B. Moore, D. Cazorla-Amorós, A. Linares-Solano, Carbon 42 (2004) 1367–1370.
[21] J. Gorka, A. Zawislak, J. Choma, M. Jaroniec, Carbon 46 (2008) 1159–1161.
[22] M. Lillo-Ródenas, D. Cazorla-Amorós, A. Linares-Solano, Carbon 41 (2003) 267–275.
[23] M. Illán-Gómez, A. Garcia-Garcia, C. Salinas-Martinez de Lecea, A. Linares-Solano, Energy Fuel 10 (1996) 1108–1114.
[24] E. Raymundo-Pinero, P. Azais, T. Cacciaguerra, D. Cazorla-Amorós, A. Linares-Solano, F. Béguin, Carbon 43 (2005) 786–795.
[25] C. Moreno-Castilla, F. Carrasco-Marin, M.V. Lopez-Ramon, M.A. Alvarez-Merino, Carbon (2001).
[26] S.-H. Yoon, S. Lim, Y. Song, Y. Ota, W. Qiao, A. Tanaka, I. Mochida, Carbon 42 (2004) 1723–1729.
[27] A.-N.A. El-Hendawy, Appl. Surf. Sci. 255 (2009) 3723–3730.
[28] P.C. Su, C.-C. Chao, J.H. Shim, R. Fasching, F.B. Prinz, Nano Lett. 8 (2008) 2289–2292.
[29] D.H. Kim, P. Karan, P. Göring, J. Leclaire, A.M. Caminade, J.P. Majoral, U. Gösele, M. Steinhart, W. Knoll, Small 1 (2005) 99–102.
[30] G. Horvath, K. Kawazoe, J. Chem. Eng. Jpn. 16 (1983) 470–475.
[31] C.G. Sonwane, S.K. Bhatia, J. Phys. Chem. B 104 (2000) 9099–9110.
[32] A. Bakandritsos, T. Steriotis, D. Petridis, Chem. Mater. 16 (2004) 1551–1559.
[33] J. Biscoe, B. Warren, J. Appl. Phys. 13 (1942) 364–371.
[34] P.M. Barata-Rodrigues, T.J. Mays, G.D. Moggridge, Carbon 41 (2003) 2231–2246.
[35] K. Sing, R. Williams, Adsorpt. Sci. Technol. 22 (2004) 773–782.
[36] K.R. Hall, L.C. Eagleton, A. Acrivos, T. Vermeule, Ind. Eng. Chem. Res. 5 (1966) 212–216.
[37] T.W. Weber, Rk. Chakravo, AIChE J. 20 (1974) 228–238.
[38] M. Sathupunya, E. Gulari, A. Jamieson, S. Wongkasemjit, Micropor. Mesopor. Mater. 69 (2004) 157–164.
[39] A.M. Taylor, R. Roy, Am. Mineral. 49 (1964) 656–659.
[40] C.H. Christensen, K. Johannsen, E. Toernqvist, I. Schmidt, H. Topsoe, C.H. Christensen, Catal. Today 128 (2007) 117–122.
[41] Y. Sun, R. Prins, Angew. Chem. Int. Ed. 47 (2008) 8478–8481.
[42] W.G. Lin, F. Wei, F.N. Gu, X. Dong, L. Gao, T.T. Zhuang, M.B. Yue, J.H. Zhu, J. Colloid Interface Sci. 348 (2010) 621–627.